ISSN 0031-918X, The Physics of Metals and Metallography, 2016, Vol. 117, No. 4, pp. 364–370. © Pleiades Publishing, Ltd., 2016.

STRENGTH AND PLASTICITY

# Constitutive Relations for Determining the Critical Conditions for Dynamic Recrystallization Behavior[1]

**J. I. Choe**

*Department of Materials Science and Engineering, Dankook University, Cheonan, 330-714 Republic of Korea*

*e-mail: jichoe@dankook.ac.kr*

Received February 11, 2014; in final form, October 13, 2015

**Abstract**—A series mathematical model has been developed for the prediction of flow stress and microstructure evolution during the hot deformation of metals such as copper or austenitic steels with low stacking fault energies, involving features of both diffusional flow and dislocation motion. As the strain rate increases, multiple peaks on the stress-strain curve decrease. At a high strain rate, the stress rises to a single peak, while dynamic recrystallization causes an oscillatory behavior. At a low strain rate (when there is sufficient time for the recrystallizing grains to grow before they become saturated with high dislocation density with an increase in strain rate), the difference in stored stress between recrystallizing and old grains diminishes, resulting in reduced driving force for grain growth and rendering smaller grains in the alloy. The final average grain size at the steady stage (large strain) increases with a decrease in the strain rate. During large strain deformation, grain size reduction accompanying dislocation creep might be balanced by the grain growth at the border delimiting the ranges of realization (field boundary) of the dislocation-creep and diffusion-creep mechanisms.

*Keywords*: hot deformation, dynamic strain aging, microstructure

**DOI:** 10.1134/S0031918X16040037

## 1. INTRODUCTION

When metals and alloys were hot-deformed, the process conditions such as temperature and strain rate cause a slight difference in the mechanical properties of the final product. Especially during hot working, the deformation of metals such as copper or austenitic steels with low stacking fault energies involves both diffusional flow and dislocation motion [1, 2]. Since the true stress–true strain relationship depends on the strain rate, the multiple peaks on the stress-strain curve decrease as the strain rate increases, and the stress rises to a single peak at a high strain rate. Grain refinement produced by dynamic recrystallization (DR*X*) is important under hot strip rolling and other tandem mill conditions. The strain is accumulated from pass to pass until it attains and exceeds the critical strain for dynamic recrystallization. As Goetz [3] revealed, dynamic recrystallization and dynamic recovery compete with each other in reducing the dislocation densities produced through plastic deformation during hot working. For metals and alloys with high stacking fault energies such as Al and Ni, dynamic recovery via easy cross slip or climb is sufficient to reduce dislocation densities below the level for the onset of dynamic recrystallization, and thus the stress-strain curve, depending on the initial grain size, displays zero or a single peak before the stress reaches its steady-state value [4]. For alloys with low stacking fault energies, however, the stress-strain behavior depends on the strain rate. Both the cross slip and climb differ due to large stacking faults, and this in turn reduces the rate of dynamic recovery. It is understood that dynamic recovery is responsible for the stress-strain behavior with zero or a single peak, whereas dynamic recrystallization affects an oscillatory nature. At a low strain rate, there is sufficient time for the recrystallizing grains to grow before they become saturated with high dislocation densities. With an increase in strain rate, the difference in stress between the recrystallized grains and the old grains diminishes, resulting in reduced driving force for grain growth and rendering smaller grains in the alloy [5]. The aim of the present study is to investigate the critical kinetic condition for the initiation of dynamic recrystallization during deformation, which includes reviewing previous micro physical models that address the relationship between recrystallized grain size and flow stress.

## 2. THEORETICAL APPROACH

### 2.1. Deformation Dynamics

The energy dissipated during deformation is usually assumed to be approximately equal to the amount of heat released. However, these quantities are not equal. The difference is small, but it plays an essential

[1] The article is published in the original.

role in plastic deformation. From a microscopic perspective, two concurrent groups of processes are responsible for the formation of the substructure during deformation [6]. The first group involves the creation and accumulation of dislocations, which can be quantities in terms of the stored energy. The second group of processes includes the various relocation processes involved in the motion, rearrangement, and annihilation of lattice defects. The two groups of processes are complementary because an increase in the rate of annihilation results in a decrease of the stored energy and vice versa [7]. A sufficient difference in stored energy is observed between the volume within the nucleus and the surroundings: these differences increase with higher strain and lower recovery. Moreover, this requirement is much greater for growth under dynamic conditions than under static conditions because the continuing straining generates a substructure behind the migrating boundary [8].

At a constant temperature, the strain required to attain this critical difference increases with increasing strain rate σ in the hot working range ($10^{-3} \sim 10^{3}$ s$^{-1}$). In contrast, in the creep range ($10^{-8} \sim 10^{-3}$ s$^{-1}$), the strain required increases with decreasing strain rate, because the problem is no longer the accumulation of a substructure in the growing grain, but the insufficient substructure outside the grain [9]. The aim of the present study is to investigate the critical kinetic condition for initiation of dynamic recrystallization during deformation, which includes reviewing previous microphysical models that generally address the relationship between recrystallized grain size and flow stress; micro-structural evolution at low strain rates is non-uniform but becomes progressively uniform as the strain rate increases. Let us consider a ductile polycrystalline phase such as copper or aluminum, capable of storing a form of mechanical energy. In a temporal sense, the conditions of instability during local deformation may be given by

$$P = \sigma S, \left(\sigma = \frac{P}{S} = \frac{F}{S}\right), \tag{1}$$

where $P$ is the compressive load and $S$ is the surface area of a tested material; the rate of change in $P$ is

$$dP = dS + Sd\sigma. \tag{2}$$

At a constant $P$, which means $dS = -Sd\sigma$, and according to the relation, which is a consequence of that in any case the differentials (positive by definition in contrast to mere changes Δ in surface area and compression deformation) $dS$ and $d\sigma$ are of opposite senses because of the volume conservation,—

$$\frac{dL}{L} = -\frac{dS}{S} = d\varepsilon = \frac{d\sigma}{\sigma}, \tag{3}$$

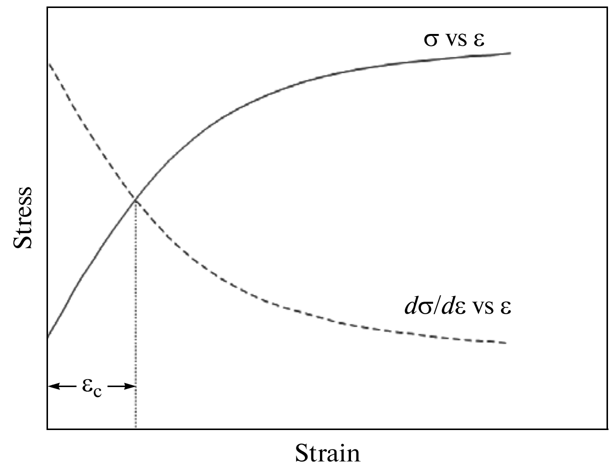


**Fig. 1.** Transformation mechanism on stress-strain curve of austenitic alloy ($\varepsilon_c$ is the critical strain).

—we have the stress-strain relationship

$$\sigma = \frac{d\sigma}{d\varepsilon}, \tag{4}$$

where $\frac{d\sigma}{d\varepsilon}$ is the conventional strain hardening rate. It can be represented as a function of the engineering strain $\tilde{e}$:

$$\frac{d\sigma}{d\varepsilon} = f(\tilde{e}), \tag{5}$$

where $\tilde{e} = \frac{L - L_0}{L_0} = \frac{L}{L_0} - 1$. Obviously,

$$\frac{L}{L_0} = 1 + \tilde{e}, \tag{6}$$

$$d\tilde{e} = \frac{dL}{L_0}. \tag{7}$$

Thus, using (3), (4), (6), and (7), we obtain

$$\frac{d\sigma}{d\varepsilon} = \frac{d\sigma}{d\varepsilon}\frac{d\tilde{e}}{d\tilde{e}} = \frac{d\sigma}{d\tilde{e}}\frac{\frac{dL}{L_0}}{\frac{dL}{L}} = \frac{d\sigma}{d\tilde{e}}(1 + \tilde{e}) = \sigma \tag{8}$$

and, finally,

$$\frac{d\sigma}{d\tilde{e}} = \frac{\sigma}{1 + \tilde{e}}. \tag{9}$$

Equations (9), as well as (4), is typical of the deformation development at $dP = 0$ that precedes the moment of the possible start of dynamic recrystallization (and shows no specific features that we are going to deal with). Figure 1 shows the critical strain $\varepsilon_c$ (note that the onset of dynamic recrystallization during hot deformation occurs when $\varepsilon_c$ is reached). In

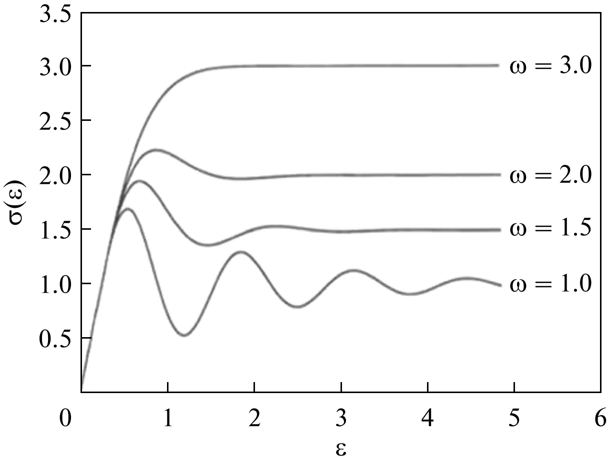


**Fig. 2.** Stress-strain relationship according to the solution of a delay differential equation (DDE).

other words, the dynamic events are the micro-structural changes that occur during the deformation [10].

In this work, various predictive models are utilized for modeling a stress-strain behavior. The approach is characteristic of the critical strain for nucleation for recrystallization and a delay time due to diffusion taken into account in terms of critical strain.

### *2.2. Stress-strain Curve with Multiple Peaks*

Hot working is a thermo-mechanical process that involves features of both diffusion flow and dislocation motion. If an insulation time is needed for the nucleation of new recrystallizing grains, for the climb of dislocations or some other event, the ongoing of recovery might depend on the deformation state at an earlier time and annealing temperature. When considering a ductile polycrystalline phase such as copper or aluminum capable of storing a form of mechanical energy, the flow stress depends on average dislocation density and evolution of dislocation format during deformation. According to Kocks [11], dislocation density ($\rho$) with respect to true strain ($\varepsilon$) may be given by

$$\frac{d\rho}{d\varepsilon} = K_1\sqrt{\rho} - K_2\rho, \tag{10}$$

where $K_1$ is the rate of dislocation storage, $K_2$ is the rate of dislocation recovery. As is known,

$$\sigma = \alpha\mu b\sqrt{\rho}, \tag{11}$$

where $\alpha$ is a materials constant, $\mu$ is the shear modulus, and $b$ is the abs. value of Burgers vector.

The Eq. (10), with taking into account (11), can be converted to an equation for the rate of change in stress $\sigma$ with respect to strain $\varepsilon$, namely,

$$\frac{d\sigma}{d\varepsilon} = 0.5\alpha\mu b K_1 - 0.5K_2\sigma. \tag{12}$$

At the steady stage of flow, when $\frac{d\sigma}{d\varepsilon} = 0$, the steady-stage stress becomes

$$\sigma_{ss} = \alpha\mu b(K_1/K_2).$$

This means that the recovery occurs instantaneously and the magnitude of softening depends only on the stress at $\varepsilon$. Therefore, from Eq. (12) one is allowed to expect that an insulation time ($t$) can be related to an insulation strain ($\varepsilon_n$) in the case that multiple peaks are not observed in the stress-strain curve under deformation at a constant strain rate ($\dot{\varepsilon}$). That is, the influence of an insulation strain on the stress-strain relationship involves a number of forms [12],

$$\frac{d\sigma}{d\varepsilon} = f\{\sigma(\varepsilon), \sigma(\varepsilon-\varepsilon_1), \sigma(\varepsilon-\varepsilon_2), \dots\}, \tag{13}$$

where $\varepsilon_1$, $\varepsilon_2$, and $\varepsilon_3$ are insulation characteristics of the alloy recovery process. For a single delay strain ($\varepsilon_n$), stress-strain variation is described by the steady-stage stress function ($\theta$) and steady-stage stress ($\omega$):

$$\frac{d\sigma}{d\varepsilon} = \theta - \frac{\theta}{\omega}\sigma(\varepsilon-\varepsilon_n). \tag{14}$$

In the limit of $\varepsilon_n = 0$, Eq. (14) becomes identical to Eq. (12), with

$$\theta = 0.5\alpha\mu b K_1,\ \omega = \sigma_{ss} = \alpha\mu b(K_1/K_2). \tag{15}$$

This equation can be solved numerically by using the same initial condition

$$\sigma(\varepsilon) = \sigma_0 \text{ (when } \varepsilon \le 0). \tag{16}$$

Substituting (16) into (14), with (15) in mind, gives

$$\frac{d\sigma}{d\varepsilon} = \theta - \frac{\theta}{\omega}\sigma_0 \ \ (0 \le \varepsilon \le \varepsilon_n), \tag{17}$$

which after integration yields

$$\sigma(\varepsilon) = \sigma_0 - \frac{\theta}{\omega}(\sigma_0 - \omega)\varepsilon \ \ (0 \le \varepsilon \le \varepsilon_n). \tag{18}$$

For the next iteration, Eq. (14) (to be integrated at $\varepsilon_n < \varepsilon < 2\varepsilon_n$) becomes

$$\frac{d\sigma}{d\varepsilon} = \theta - \frac{\theta}{\omega}\left[\sigma_0 - \frac{\theta}{\omega}(\sigma_0 - \omega)(\varepsilon - \varepsilon_n)\right], \tag{19}$$

where the steady-stage stress $\omega$ can be considered as a functional parameter implicitly dependent on the experimental strain rate $\dot{\varepsilon}$, i.e., $\omega = \omega(\dot{\varepsilon})$... And so on, ad infinitum.

The flow stress behavior of the DD equation is presented in Fig. 2, where $\omega$ varies from 3, 2, and 1.5 to 1 for a case with $\theta = 4$, $\varepsilon_n = 0.3$, and $\sigma_0 = 0$. Figure 2 shows that the flow curve begins to oscillate at a low $\omega$, and the number of stress peaks increases with a decrease in $\omega$. Regardless of the oscillation, the stress approaches a steady-stage value set equal to $\omega$. A sta-

Chemical composition of 99.92% electrolytic copper

| | P | Sn | Pb | Ni | Ag | Fe | Zn | Sb | S | O |
|---|---|---|---|---|---|---|---|---|---|---|
| ppm | 253 | 120 | 169 | 54.3 | 46.5 | 16.3 | 31.3 | 25 | 9.8 | 46 |

bility analysis shows that when $\lambda = (\theta\varepsilon_n/\omega) \leq (1/e) = 0.37$, the stress $\sigma$ increases monotonically from $\sigma_0$ to $\sigma_{ss} = \omega$. When $1/e < \lambda < \frac{\pi}{2} = 1.57$, the stress displays an oscillatory behavior with decaying amplitude; at $\lambda = \frac{\pi}{2}$, the oscillation becomes perpetual with a period equal to $4\varepsilon_n$. In Fig. 2, $\lambda$ is equal to 0.4, 0.6, 0.8, and 1.2 for $\omega = 3$, 2, 1.5, and 1, respectively. In rheology theory, Eq. (14) with $\varepsilon_n = 0$ describes the stress-strain relationship for a linear spring dashpot model, in which $\theta$ becomes the spring constant and $\omega$ is equal to $3\eta\dot{\varepsilon}$, where $\eta$ is the viscosity of the dashpot [1]. For hot working, $\theta$ represents a high temperature modulus. For an alloy with low stacking fault energy, the low strain rates provide adequate time for the recrystallizing grains to grow before they become saturated with high dislocation density [13]. Thus, the final average grain size at the steady stage (large strain) increases with a decrease in the strain rate ($\dot{\varepsilon}$).

Table shows the chemical composition of 99.92% electrolytic copper. True stress-strain curves of electrolytic copper B (B means that Cu B has 46 ppm of oxygen) obtained at 650 and 850°C and at different strain rates [14] are shown in Figs. 3a and 3b.

In Fig. 3a, the strain rate below 0.03 $s^{-1}$ exhibited a peak during initial deformation followed by steady stage flow. At a strain rate lower than 0.01 $s^{-1}$, multiple peaks occurred before the steady stage was reached. At strain rates higher than 0.1 $s^{-1}$, the curves exhibited a strain hardening feature. On the other hand, in the higher temperature range of 750–950°C, the flow curves exhibited softening at all strain rates (typically shown for 850°C in Fig. 3b).

The beginning of dynamic recrystallization (noticeable softening after the peak stress) was first noticed on the hot flow curve at 650°C and 0.03 $s^{-1}$ for electrolytic copper. Subsequent peak stresses after the maximum stress peak (cyclic or multiple peak dynamic recrystallization) were noticed at the slowest strain rate at 850°C on the hot flow curve (see Fig. 3b).

Dynamic recrystallization was only of single peak type at the highest strain rates (0.3, 0.1 $s^{-1}$) at these temperatures, which is a general feature typical of the dynamic recovery case. Figure 3 shows the stress-strain curves obtained from the experimental test and the critical (delay differential equation) data [14]. It seems fair to conclude that the DD equation shows most of the basic physics associated with the flow behavior of metals and alloys during hot working, especially of metals and alloys with low stacking fault energies [14]. Clearly, further testing of the model is needed for improvement.

### 2.3. Dynamically Recrystallized Microstructure

In order to describe the microstructure evolution, the main input parameters of the models are the deformation parameters ($\varepsilon$, $\dot{\varepsilon}$, $T$), the pauses parameters ($t$ and $T$), and grain size ($D$). The output parameters include the recrystallization fraction $X$, the time $t_{0.5}$ (strain $\varepsilon_{0.5}$) for 50% recrystallization, and the critical strain $\varepsilon_c$, etc. [15].

However, the integration of the recrystallization model into the flow stress based on the dislocation theory is hampered by different types of recrystalliza-

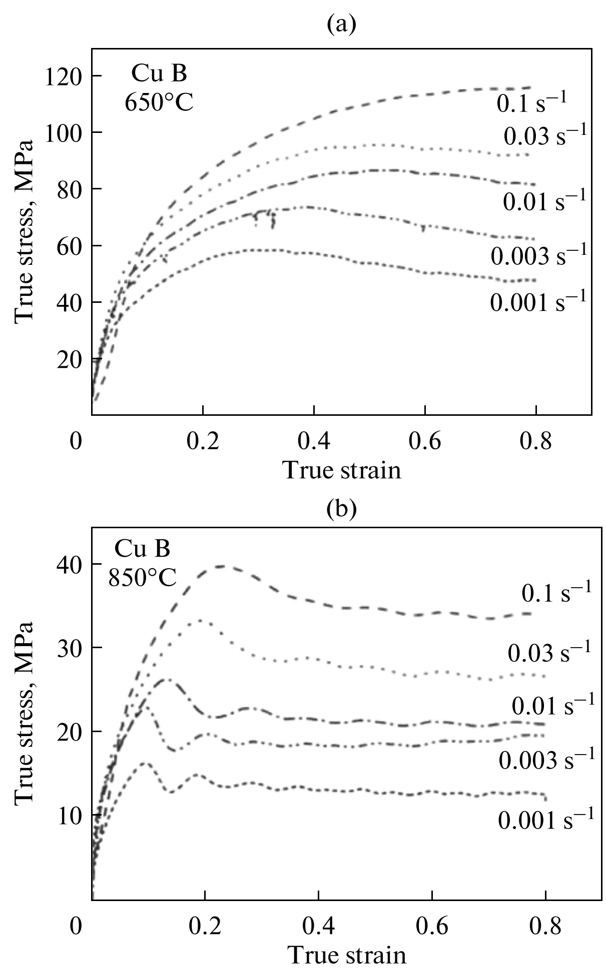


**Fig. 3.** Hot compression curves of Cu at (a) 650°C, (b) 850°C, and different strain rates [14].

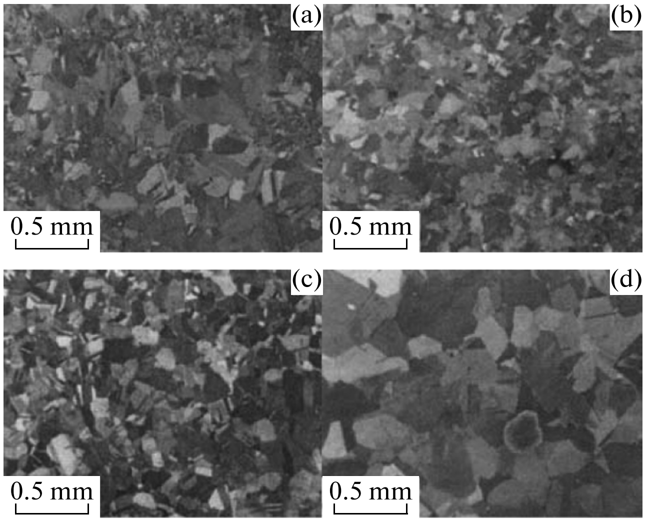


**Fig. 4.** (a) After 650°C, 0.3 $s^{-1}$ and $\varepsilon = 0.8$, (b) after 650°C, 0.001 $s^{-1}$ and $\varepsilon = 0.8$, (c) after 850°C, 0.3 $s^{-1}$ and $\varepsilon = 0.8$, (d) after 850°C, 0.001 $s^{-1}$ and $\varepsilon = 0.8$ [14].

tion. From Johnson–Mehl–Avrami theory [16], the recrystallization in a two stage process is considered, which consists of the nucleation and the grain growth. The nuclei are meant to occur only during deformation. Then, the difference between a dynamic recrystallization (DR*X*) and other types of recrystallization was in the fraction of the new grain while incorporating deformation data. The final microstructure after 0.80-*t* strain was refined for electrolytic coppers, even though some coppers were subjected to multiple peaks in the DR*X*. The micrograph of Fig. 4 shows the final microstructure after hot compressing from 650 and 850°C at different strain rates. The micrographs at a lower temperature and higher strain rates show incomplete DR*X*, even though the onset of DR*X* from the hot flow curve was not evident. The dynamically recrystallized grain size was smaller as the strain rate increased. For example, by observing the micrographs in Fig. 4, it can be seen that the microstructure is finest for 0.3 $s^{-1}$ and is coarsest for 0.001 $s^{-1}$. Therefore, for the conditions under which the complete DR*X* takes place, a coarser microstructure was the typical trend as the strain rate was slower.

Introduce the constant $\beta$, which is dependent on temperature and grain size. Subgrain boundaries produced during hot working are strain rate sensitive and thus the average subgrain size may increase with increasing strain at a certain strain rate. Taking temperature effects into consideration, we utilize a creep power law type and write

$$\omega = A\dot{\varepsilon}^m \exp\left(\frac{m\theta}{RT}\right) = \beta\dot{\varepsilon}^m, \tag{20}$$

where $A$ is the dimensional ([$\sigma$]) pre-exponential constant, $Q$ is the activation energy for self diffusion, $m$ is the strain rate sensitivity, and $\beta$ represents (as was mentioned above) dimensional ([$\sigma$]) constants whose values depend on temperature and grain size. It is obvious that $\ln\omega = \ln\beta + m\ln\dot{\varepsilon} = \ln\sigma_{ss}$, where according to (15)

$$\omega = \sigma_{ss} = \alpha\mu b(K_1/K_2) = \frac{\theta\varepsilon_n}{\lambda} = 3\eta\dot{\varepsilon}.$$

Thus, for the flow stress at the steady stage (ss), (with deleted but implied sub indices "ss") we have $\sigma = \beta\dot{\varepsilon}^m$. In going to differentials in the equation $\ln\sigma = \ln\beta + m\ln\dot{\varepsilon}$, namely, $d\ln\omega = md\ln\dot{\varepsilon}$, we obtain for $m$ the expression

$$m = \frac{d\ln(\sigma/\beta)}{d\ln\dot{\varepsilon}}; \tag{21}$$

thus, $m$ can be determined as the slope of a logarithmic plot of the measured stress versus strain rate. Keeping in mind an expression for the strain rate in the dislocation creep

$$\dot{\varepsilon} = K_3\sigma^n e^{-\frac{Q}{RT}}, \tag{22}$$

where $K_3$ is the material constant and $n$ is the grain-size-insensitive (GSI) power law exponent constant (both determined from (20)), for the dependence of the recrystallized grain size $D$ on the flow stress at the steady stage, one can obtain [17]

$$D = K_4\sigma^{-m} e^{\frac{\Delta Q}{RT}}, \tag{23}$$

where $K_4$ is the material constant, $m$ is determined in (21), and $\Delta Q$ is proportional to the difference between the activation energies for the bulk and the grain boundary diffusion.

The development of a steady stage subgrain structure involved a dynamic balance between the flux of dislocations gliding and climbing into subgrain walls and the climb controlled annihilation of dislocation at the nodal point in the subboundary network [17]. Accordingly, the relationship between the subgrain size $d_s$ and flow stress $\omega$ at a steady stage is determined by the product of dislocation generation rate and mean slip distance, and by the climb velocity in the subgrain wall. The flux term is directly related to the creep behavior of the material, whereas the nodal annihilation term embodies the diffusivity for climb in subboundaries. Figure 5a shows grain size reduction by dynamic recrystallization or grain growth on the stress-strain curve for 6/4 Brass at 600°C from McQueen and Baudelet [18]. Associated with this evolution, a balance is required between grain size reduction and grain growth, at a reduced stress compared with the flow stress required for dislocation creep without recrystallization at the same strain and temperature. In Fig. 5b, the high temperature stress-strain curve with a clean peak followed by weakening

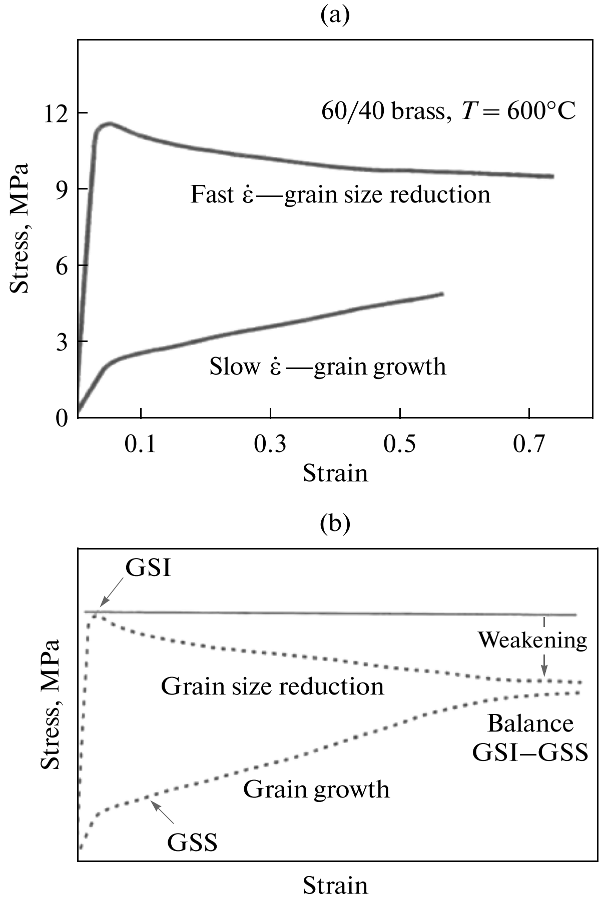


**Fig. 5.** (a) Stress-strain curves for 60/40 brass at $T = 600°C$ from McQueen and Baudelet (1980), showing weakening during grain size reduction at fast strain rate, and hardening caused by grain coarsening at slow strain rate. (b) Possible interpretation of the stress-strain curves of (a), in terms of the field boundary hypothesis. At high stress and high strain rate, deformation starts from a single dislocation creep (GSI) mechanism, and evolves towards simultaneous control by GSI and GSS mechanisms, producing minor weakening after a peak stress. Conversely, at sufficiently low stress and strain rates, the material initially deforms by the diffusion creep (GSS) mechanisms, until grain growth results in an increased contribution of dislocation processes and, eventually, in dual mechanism control once again [17].

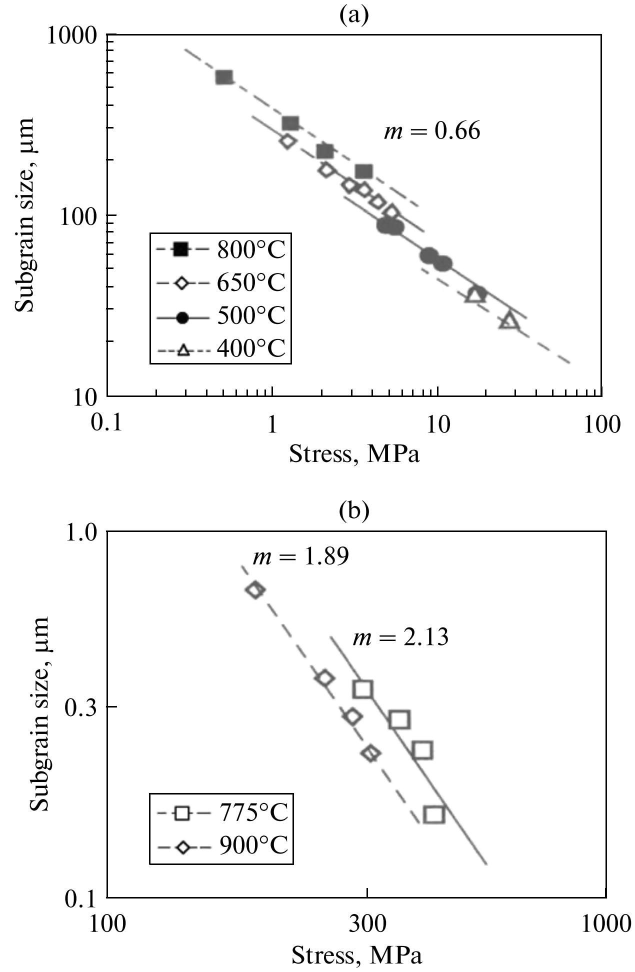


**Fig. 6.** Subgrain size data plotted versus flow stress for (a) α-Fe and (b) stainless steel 316, from data of Streby and Reppich (1973) [21] and Young and Sherby (1973) [22], respectively.

might accordingly be interpreted as demonstrating the onset of steady stage dislocation creep peak stress, followed by dynamic recrystallization and strain softening until a balance has been achieved between grain size reduction and grain growth at conditions corresponding to the dislocation creep and diffusion creep (GSS, i.e., grain-size-sensitive) field boundary. The process other than dynamic recrystallization can result in material (GSI) weakening, according to Rutter (1999) [19], such as geometrical softening caused by the development of a crystallography or recrystallized grain. That is, the investigation of recrystallization should thus include deformation tests on fine grained starting material in order to test for the progressive evolution suggested in Fig. 5. It is assumed that the nucleation rate depends on the strain $\varepsilon$, the strain rate $\dot{\varepsilon}$, the temperature $T$, and the grain size $D$.

Figure 6 shows evidence for a temperature dependence of subgrain size versus stress relation as has been already represented for α-Fe (Fig. 6a, Orlova, 1972) [20] and stainless steel 316 (Fig. 6b, Sherby, 1973) [21]. Thus, at a constant stress, the subgrain size was observed to be larger if the deformation temperature was higher. This suggests that at a constant stress and increasing temperature, the subgrain size increases. It was found that the expected increase depended on applied stress (at $m = 0.66$, see Fig. 6a), which was a direct parameter dependent on temperature.

## 3. SUMMARY

A series mathematical model has been developed for prediction of the flow stress and microstructure evolution during hot deformation. Multiple stress peaks should appear when a large ratio of the characteristic strain occurs for nucleation of recrystallization to the characteristic strain for completion of recrystallization. The model, expressed in the DD equation, displays most of the basic physics associated with the flow behavior of metals and alloys during hot working, especially those with low stacking fault energies; low strain rates provide adequate time for the recrystallized grains to grow before they become saturated with high dislocation density. Thus, the final average grain size at the steady stage (large strain) increases with a decrease in the strain rate. During large strain deformation, grain size reduction accompanying dislocation creep might be balanced by grain growth at the (virtual) boundary between dislocation creep and diffusion creep. The $D - \sigma$ relationship at a steady stage will then correspond to the equation delineating the creep field boundary and in general will be temperature dependent and in the form of $D = K_4\sigma^{-m}e^{\frac{\Delta Q}{RT}}$ (23) with $\dot{\varepsilon} = K_3\sigma^n e^{-\frac{Q}{RT}}$ (22).

## ACKNOWLEDGMENTS

The author is grateful to Professor J.K. Lee at Michigan Technological University, USA for the initiation of this study and Dr. A. Pirogov at the Institute of Metal Physics RAS, Russia for fruitful discussion and valuable help.

## REFERENCES

1. N. E. Dowling, *Mechanical Behavior of Material* (Prentice Hall, Englewood Cliffs, NJ, 1993).
2. A. K. Mukgerjee and R. H. Mishra, "Creep mechanism in dispersion strengthened materials," *Proc. The Johannes Weertman Symposium, TMS, Warrendale, PA*, **119**, 111–121 (1996).
3. R. L. Goetz and V. Seetharaman, "Modeling dynamic recrystallization using cellular automata," Scr. Mater. **38**, 405–413 (1998).
4. R. Ding and Z. X. Guo, "Coupled quantitative simulation of microstructural evolution and plastic flow during dynamic recrystallization," Acta Mater. **49**, 3163–3175 (2001).
5. J. H. P. De-Bresser, J. P. J. Reijs, and C. J. Spiers, "On dynamic recrystallization during solid state flow: Effects of stress and temperature," Geophys. Res. Lett. **25**, 3457–3460 (1998).
6. S. S. Dmytro, "The coupled model of a microstructure evolution and a flow stress based on the dislocation theory," ISIJ Int. **45**, 1187–1193 (2005).
7. F. Grosman, "Application of a flow stress function in programmes for computer simulation of plastic working processes," J. Mater. Process. Techn. **64**, 169–180 (1997).
8. C. Roucoules, M. Pietrzyk, and P. D. Hodgson, "Analysis of work hardening and recrystallization during the hot working of steel using a statistically based internal variable model," Mater. Sci. Eng., A **339**, 1–9 (2003).
9. E. J. Mittemeijer and F. Sommer, "Solid state phase transformation kinetics: A modular transformation model," Z. Metallkd. **93**, 352–361 (2002).
10. W. Roberts, *Deformation Processing and Structure* (ASM, Metals Park, OH, 1984), pp. 109–121.
11. U. F. Kocks, "Laws for work-hardening and low-temperature creep," J. Eng. Mater. Technol. **98**, 76–85 (1976).
12. I. R. Epstein, "Differential delay equations in chemical kinetics: Some simple linear model systems," J. Chem. Phys. **92**, 1702–1712 (1990).
13. L. Zhang, W. Yang, and Z. Sun, "Modeling of microstructural evolution during dynamic recrystallization in coarse Nb microalloyed austenite," J. Univ. Sci. Techn. Begin. **14**, 130–135 (2007).
14. V. G. Garcia, J. M. Cabrera, and J. M. Predo, "Predicting multiple peak dynamic recrystallization of copper," Mater. Sci. Forum **467**, 1181–1186 (2004).
15. A. P. Singh, D. Sengupta, G.M.D. Murthy, S. Jha, M. P. Yallasiri and N. S. Mishra, "A mathematical model to predict microstructural changes and final mechanical properties of API-grade steel plates produced by thermomechanical control processing," *Proc. 44th Mech. Working Steel Proc. Conf. Warrendale, PA, 2002*, pp. 1139–1141.
16. W. A. Johnson and R. F. Mehl, "Reaction kinetics in processes of nucleation and growth," TMS–AIMME **135**, 416–458 (1939).
17. J. H. P. De-Bresser, J. H. Ter-Heege, and C. J. Spiers, "Grain size reduction by dynamic recrystallization: Can it result in major rheological weakening?" Int. J. Earth Sci. **90**, 28–45 (2001).
18. E. H. Rutter, "Experimental study of the influence of stress, temperature, and strain on the dynamic recrystallization of carrara marble," J. Geophys. Res. **100**, 24651–24663 (1995).
19. H. J. McQueen and B. Baudelet, "Comparison and contrast of mechanisms, microstructures, ductilities in superplasticity and dynamic recovery and dynamic recrystallization," in *Strength of Metals and Alloys (Proc. 5th Int. Conf. on Strength of Metals and Alloys)*, Ed. by P. Haasen, V. Cerold, and G. Kostorz, (Pergamon, Aachen, 1980), pp. 329–336.
20. A. P. Orlova and J. Cadek, "Dislocation structure and applied, effective and internal stress in high-temperature creep of alpha iron," Philos. Mag. **25**, 865–877 (1972).
21. G. Streb and B. Reppich, "Steady state deformation and dislocation structure of pure and Mg-doped LiF single crystals. II. Etch pit studies of dislocation structure," Phys. Status Solidi A **16**, 493–505 (1973).
22. O. D. Sherby, "Subgrain formation and boundary strengthening in iron based materials," J. Iron Steel Inst. **211**, 640–646 (1973).